Research Journal of Environmental Sciences

ISSN 1819-3412

Academic
Journals Inc.

www.academicjournals.com

OPEN ACCESS Research Journal of Environmental Sciences

ISSN 1819-3412
DOI: 10.3923/rjes.2018.220.228

Research Article
Preparation and Photocatalytic Activity of AG_3PO_4/MCM-41 Nanocomposite for Degradation of Organic Compounds in Aqueous Solution

Golnaz Heydari, Hadi Fallah-Moafi and Mohammad Ali Zanjanchi

Department of Chemistry, Faculty of Science, University of Guilan, P.O. Box 1914, Rasht, Iran

Abstract

Background and Objective: Dispersion of silver compounds onto appropriate support is an adequate procedure for fabricating active photocatalysts for degradation of environmental pollutants. The current study investigated the dispersion of AG_3PO_4 as potential photocatalyst onto MCM-41 as a mesoporous support. **Materials and Methods:** The disodium hydrogen phosphate was found to be an appropriate source of phosphate for the synthesis of AG_3PO_4/MCM-41. Two different procedures of post-synthesis and during-synthesis methods were used for preparation of the photocatalysts. Accurate structural and analytical methods were used for characterization of the prepared photocatalysts. **Results:** The XRD results revealed that all the materials showed a body-centered cubic crystal structure. Maximum Elimination of methylene blue dye was found within 15 min, in slightly acidic media in the presence of photocatalyst. Pseudo first order was the best fitted model for this study. **Conclusion:** The post-synthesized AG_3PO_4/MCM-41 showed the highest capability for elimination of methylene blue and 2,4-dichlorophenol. Part of this capability for elimination of methylene blue is due to its adsorption onto the photocatalyst.

Key words: AG_3PO_4/MCM-41, wastewater treatment, photocatalyst, methylene blue and 2,4-dichlorophenol, advanced oxidation, silver compounds, mesoporous support

Citation: Golnaz Heydari, Hadi Fallah Moafi and Mohammad Ali Zanjanchi, 2018. Preparation and photocatalytic activity of AG_3PO_4/MCM-41 nanocomposite for degradation of organic compounds in aqueous solution. Res. J. Environ. Sci., 12: 220-228.

Corresponding Author: Hadi Fallah Moafi, Department of Chemistry, Faculty of Science, University of Guilan, P.O. Box 1914, Rasht, Iran

Competing Interest: The authors have declared that no competing interest exists.

Data Availability: All relevant data are within the paper and its supporting information files.

INTRODUCTION

Heterogeneous photocatalysis is considered as an advanced and effective approach for the removal of organic pollutants from wastewater sources. Therefore, development of the efficient, sustainable and visible-light-reactive photocatalytic materials remains a challenge. During the last decade an increasingly great number of new materials have been synthesized and examined as promising photocatalysts[1,2]. These materials are different compounds or composites with distinct composition and structure. Among these visible light sensitive photocatalysts, some containing Bi_2WO_6[3,4], $BiVO_4$[5,6] and AG_3PO_4[7-9] have currently been investigated and exploited. They have shown relatively good performance for degradation of certain pollutants. For enhancement of the photochemical reactivity of them certain approaches are utilized. For example, various techniques including structure control[10], hetero-coupling[11-14] and plasmon assist[15] have been employed to modify AG_3PO_4 for better functioning. As is known, photocatalytic reaction is carried out on the semiconductor surface and the morphology as well as the extent of the exposed area have great influence on photocatalytic efficiency. Therefore, great attention has been devoted to the surface engineering to obtain materials with higher photoactive properties. Supporting AG_3PO_4 on the mesoporous materials is a fascinating alternative for surface engineering[16-18]. This requires considerable attention because ordered mesoporous materials have enormous surface area, adjustable pore size and limited pore size distribution[19,20]. One of the most utilized mesoporous materials is MCM-41 which is an inorganic silica based material and exhibits a uniform hexagonal arrangement of cylindrical pores. In this contribution, this study designed a new composite photocatalyst by supporting AG_3PO_4 onto MCM-41. Two different procedures for preparation of these photocatalysts were used and tested them for the efficient degradation of methylene blue (MB) and 2,4-dichlorophenol (DCP). Present results showed that the photocatalytic activity of the post-synthesized AG_3PO_4/MCM-41was remarkably better than pure AG_3PO_4 nanoparticles.

MATERIALS AND METHODS

Reagents and materials: Tetraethyl orthosilicate (TEOS) was purchased from ACROS. N-cetyltrimethylammonium-bromide (CTMABr), ethylamine, ethanol, methylene blue, 2,4-DCP, NH_3, HCl, $Na_2HPO_4{\cdot}12H_2O$, $AGNO_3$ were obtained from Merck.

Preparation of MCM-41: The mesoporous MCM-41 was synthesized as described in previous report[21]. The TEOS was used as a source of silicon and CTAB was used as template for preparation of MCM-41. The procedure for the synthesis is described briefly: 2.7 g ethylamine was added to 45ml of deionized water and the mixture was stirred at room temperature for 10 min. Then, 1.48 g of CTAB was gradually added to the solution under stirring and stirring was continued for 30 min until a clear solution was resulted. Then, 2.1 g TEOS was added drop wise to this solution. The molar composition of the mixture was:

$$SiO_2{:}1.6\ EA{:}0.215\ CTAB{:}125\ H_2O$$

The pH of the reaction mixture was adjusted to 8.5 by adding of hydrochloric acid solution (1.0 M) to the mixture. At this stage, the precipitate was formed. After 2 h, under stirring, the precipitate was separated and washed by centrifugation. The sample was dried at 45°C for 12 h. The prepared MCM-41 was calcined at 550°C for 5 h to decompose the template. The product was collected as a white powder form.

Preparation of AG_3PO_4/MCM-41: The nano-structured AG_3PO_4/MCM-41 materials were synthesized using hydrothermal method. Addition of AG_3PO_4 to the structure of MCM-41 was performed in two different ways. In the first approach the prepared MCM-41 was added to the synthesis composition of AG_3PO_4. This procedure was called as a Post-Synthesis method. In the second approach the precursors for preparation of MCM-41 were added to the solution containing silver nitrate and disodium hydrogen phosphate. This procedure was called a During-Synthesis method. As a typical procedure, in the first method 5.1 g silver nitrate and 0.036 g CTAB were added into 40 mL of deionized water to form solution 1. To 10 mL of deionized water, 2.7 g disodium hydrogen phosphate was added and then the solution was heated to 40°C with continuous stirring for 30 min. Then, 0.5 g of the calcined MCM-41 was added into this solution. This suspension was then added into solution 1 with continuous stirring for 30 min to form yellow colloidal solution. The mixture was stirred at room temperature for 60 min. The solid was then collected by filtration. Finally, the obtained powder were dried in an oven at 100°C and then calcined in air at 450°C for 4 h. This sample was designated as AG_3PO_4/MCM-41(PS). In the second procedure, 5.1 g silver nitrate and 0.036 g cetyltrimethylammonium bromide (CTMABr) were added into 40 mL of deionized water to form

solution 1. To 10 mL of deionized water, 2.7 g disodium hydrogen phosphate was added and then the solution was heated to 40°C with continuous stirring for 30 min to form solution 2. Solution 2 was then added into solution 1 with continuous stirring while adding TEOS. Other steps were replication such as those mentioned for the preparation of the pure MCM-41. This sample was designated as AG_3PO_4/MCM-41(DS). A pure AG_3PO_4 sample was also prepared for comparison with AG_3PO_4/MCM-41 samples of present research.

Characterization: A Philips PW1840 X-ray diffractometer with Cu Kα radiation were used to obtain the powder XRD patterns. A Mira 3-XMU field-emission scanning electron microscope (FESEM) was used to observe the morphology and size of the prepared samples. The energy-dispersive X-ray spectrometry (EDS) was performed to obtain the chemical compositions of the samples. The UV-vis diffuse reflectance spectra (DRS) of the samples were recorded within the wavelength range of 400-700 nm by a Shimadzu UV-2100 spectrophotometer equipped with an integrating sphere attachment. $BaSO_4$ was used as a reflectance standard.

The photochemical reactor was a beaker containing suspension of MB or DCP solutions and the solid photocatalyst. It was placed in a ventilated chamber elaborated in laboratory. The suspension was magnetically stirred during the course of irradiation. The UV radiation was carried out with a 400 W Krypton lamp (Osram) and visible illumination was performed with a 100 W tungsten lamp (Toshiba). The irradiation range of the UV lamp is 90% in the UV-A (400-315) and 10% in the UV-B (315-280 nm) region. The distance between the lamp and the reactor is about 30 cm for all the experiments. Before starting to irradiation, the sample was stirred in the dark for 15 min to establish an adsorption-desorption equilibrium between the photocatalyst surface and MB (or DCP). Following irradiation, regular sampling and removal of the photocatalyst particles by centrifugation, the concentration of the residual MB or DCP were analyzed by spectrophotometric method. A Shimadzu UV-2100 spectrophotometer was employed for the measurement of the concentration. All the experiments were conducted at room temperature. The aqueous MB/catalyst or DCP/catalyst suspensions were prepared by the addition of 50 mg catalysts to 50 mL aqueous solution of the probe pollutant when a visible light irradiation was exploited. For the UV degradation experiment, less amount of the catalyst (30 mg) was used. The initial concentration of MB and DCP was 20 mg L^{-1} in each experiment. A neutral media of pH about 7 was used in all the experiments.

RESULTS AND DISCUSSION

Structural analysis

XRD analysis: The low angle XRD patterns for MCM-41 and the calcined MCM-41 were shown in Fig. 1. The diffraction patterns showed typical low angle characteristic reflections for MCM-41[22]. These correspond to the planes 100, 110, 200 and 210 respectively. The weaker reflections corresponding to the planes 110, 200 and 210 could hardly be seen for the calcined MCM-41 (Fig. 1b). The frequent disappearing of these weak reflections has been assigned to disordering of the array of meso channels of MCM-41 samples which had suffered the calcination step[23]. The small shift of the main diffraction peak toward higher 2θ for the calcined MCM-41is because of the shrinkage of the structure which has happened because of the template removal due to calcinations[24].

The XRD patterns of the prepared photocatalysts (AG_3PO_4/MCM-41 (PS), AG_3PO_4/MCM-41 (DS) and the pure AG_3PO_4) are shown in Fig. 2. Several diffraction peaks can be identified which are consistent with those of body-centered cubic structure of standard AG_3PO_4 (JCPDS No. 06-0505). Presence of these XRD reflections confirmed that parts of AG_3PO_4 crystals were embedded inside pores or onto surface of MCM-41. There are also a few other diffraction peaks in AG_3PO_4/MCM-41(DS) which are not belong to AG_3PO_4, designated them with a Δ symbol in Fig. 2c. They were most probably due to AGBr which could be formed during our synthesis procedure for preparation of AG_3PO_4/MCM-41(DS). This identification for AGBr was based on JCPDS Card no. 06-0438. Presence of AGBr could be the result of little

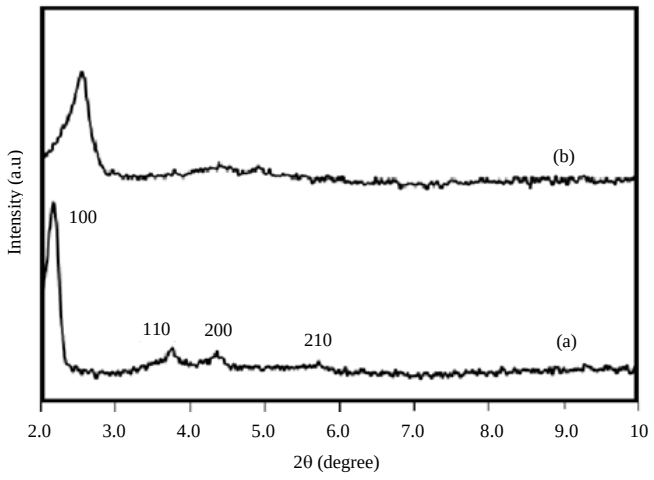

Fig. 1(a-b): Powder XRD patterns for MCM-41 samples, (a) As-synthesized MCM-41 and (b) Calcined MCM-41

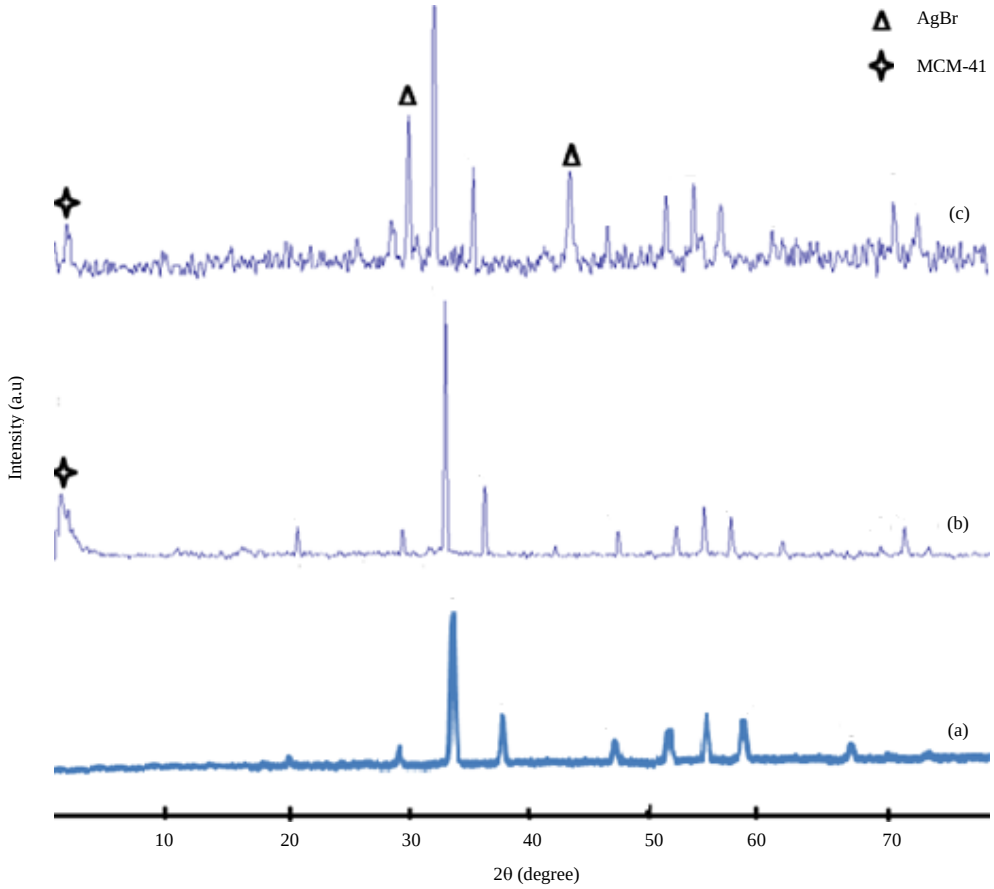

Fig. 2(a-c): Powder XRD patterns for, (a) AG_3PO_4, (b) AG_3PO_4/MCM-41(PS) and (c) AG_3PO_4/MCM-41(DS)

solubility of AG_3PO_4 and/or presence of free AG^+ in the synthesis medium reacted with bromide of the template species. This is not outlying that part of bromide may be remained as occluded or adsorbed anions in MCM-41 following the subsequent calcination.

Morphological and compositional analysis: The SEM micrographs of the prepared samples are shown in Fig. 3. The MCM-41 samples consisted of agglomerates of particles with different sizes about 30-50 nm. The distribution of AG_3PO_4 into the composites cannot be distinguished easily from the SEM micrographs unless in some parts they are appeared separately and irregular. As it is observed from Fig. 3a when AG_3PO_4 is synthesized on its own it was crystallized as nano-flakes with an average thickness of 40-100 nm.

Figure 4a and b showed the spectra of the EDX analysis of AG_3PO_4/MCM-41(PS) and AG_3PO_4/MCM-41(DS), respectively. Both of them clearly showed the presence of silicon, phosphorous and silver in the structures. However, Fig. 4b showed additional signal due to bromine which arose in AG_3PO_4/MCM-41(DS). This was in accord with the XRD data described above which indicated reflection of AGBr (Fig. 2c) in the X-ray diffraction pattern of AG_3PO_4/MCM-41(DS).

DRS study: The light-absorbance property of AG_3PO_4, MCM-41, AG_3PO_4/MCM-41(PS) and AG_3PO_4/MCM-41(DS) were checked by UV–vis diffuse reflectance method, as shown in Fig. 5. The pure AG_3PO_4 showed absorption band with a maximum around 500 nm. Clearly, the pure white powder MCM-41 does not absorbed visible light and therefore appears as straight line with no peaks (Fig. 5d). The AG_3PO_4/MCM-41(PS) and AG_3PO_4/MCM-41(DS) exhibited the same maxima as AG_3PO_4 but with lower intensity compared to that of AG_3PO_4. This was reasonable because the light-absorbing materials (AG_3PO_4) were consisted only part of these composites. By extrapolating the straight line to the x-axis in this plot, Eg of the AG_3PO_4, AG_3PO_4/MCM-41(DS) and AG_3PO_4/MCM-41(PS) were estimated to 2.4, 2.3 and 1.9 eV, respectively.

Photocatalytic activity measurement: The Photocatalytic performances of the prepared photocatalysts under visible light irradiation are shown in Fig. 6 for degradation of MB.

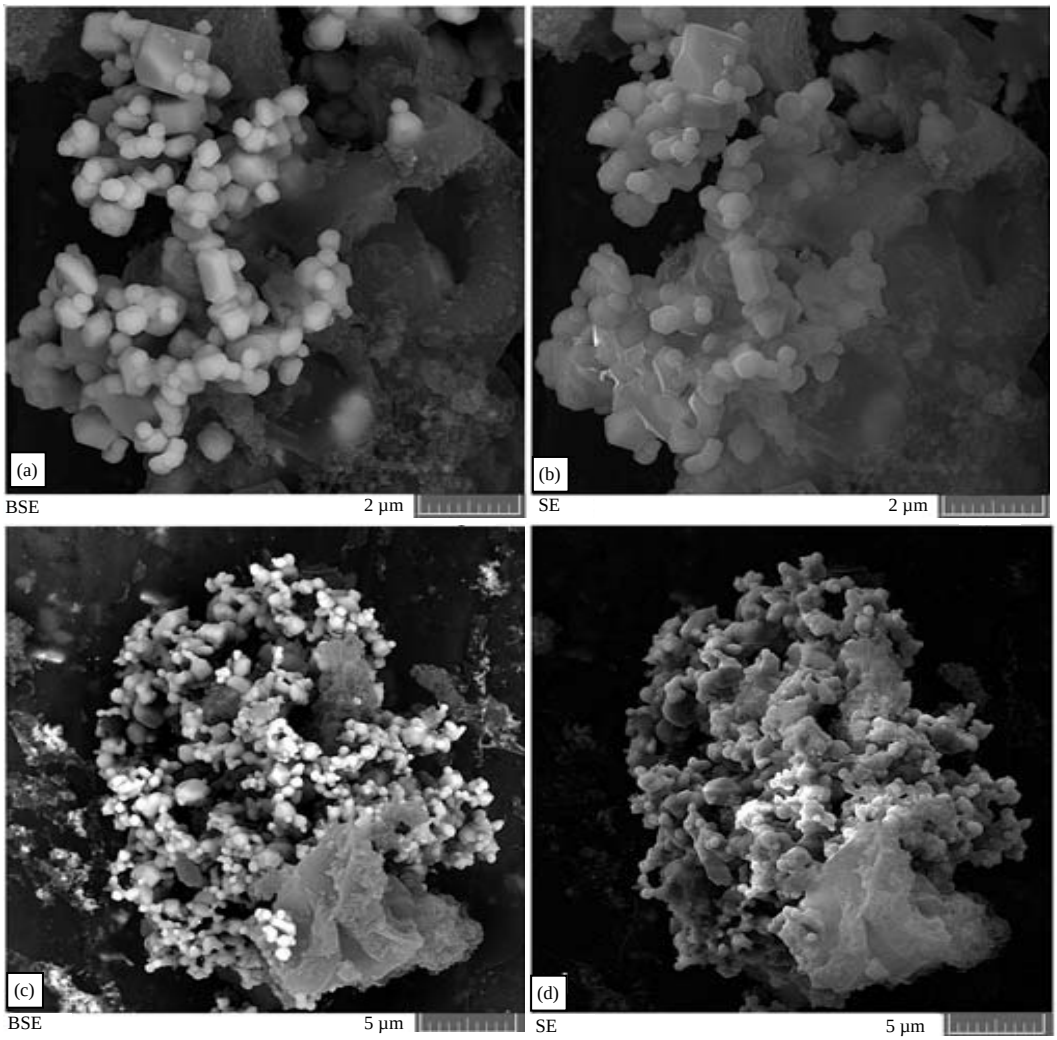

Fig. 3(a-d): Scanning electron micrographs for (a, b) AG_3PO_4 and (c, d) AG_3PO_4/MCM-41(PS).
BSE: Back-scattered electrons and SE: Secondary electrons respectively

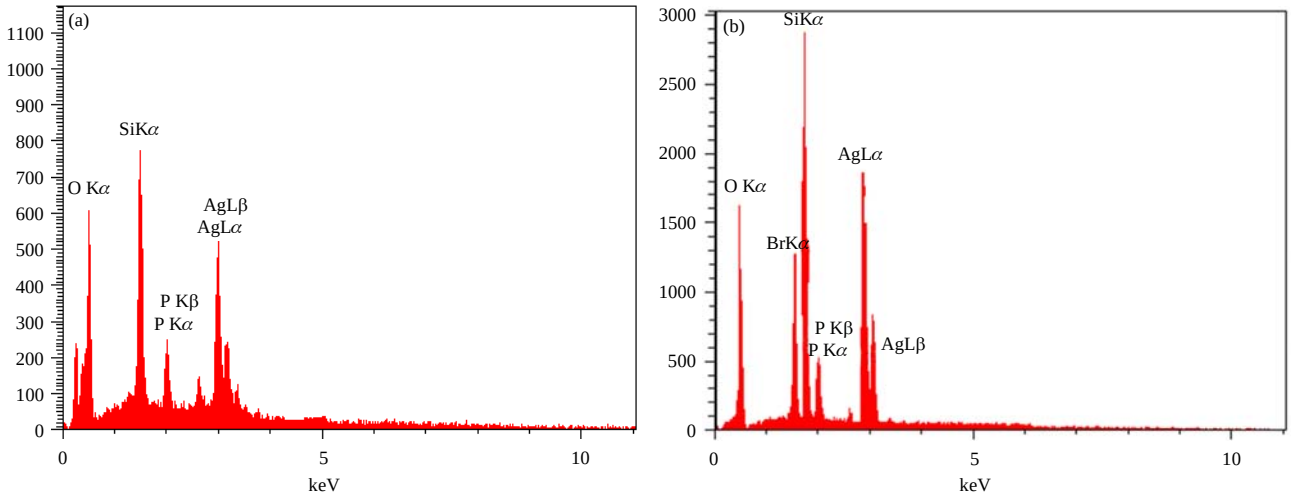

Fig. 4(a-b): EDX analysis of (a) AG_3PO_4/MCM-41 (PS) and (b) AG_3PO_4/MCM-41(DS)

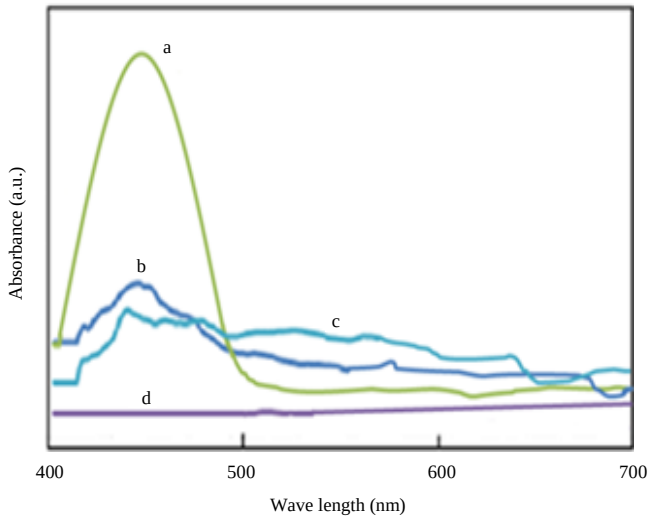

Fig. 5: UV-vis diffuse reflectance spectra of (a) AG_3PO_4, (b) AG_3PO_4/MCM-41(DS), (c) AG_3PO_4/MCM-41(PS) and (d) MCM-41

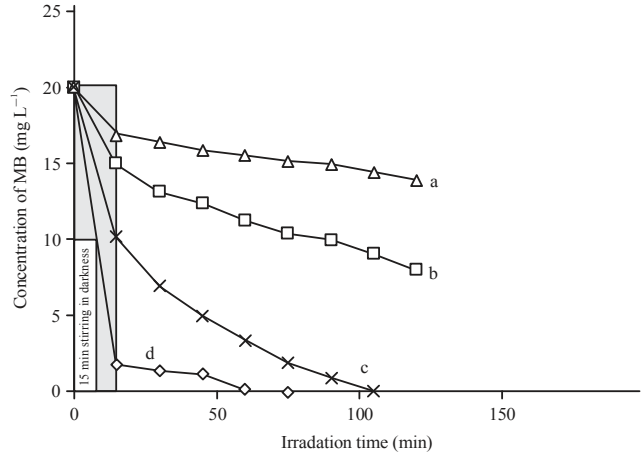

Fig. 6: Concentration changes of methylene blue as a function of irradiation time for (a) MCM-41, (b) AG_3PO_4/MCM-41(DS), (c) AG_3PO_4 and (d) AG_3PO_4/MCM-41(PS). The shaded area shows decline of concentration of methylene blue due to adsorption at the first 15 min stirring in dark. The initial concentration of MB was 20 mg L^{-1}, the weight of catalyst was 50 mg, volume of the dye solution 50 mL, photocatalytic reaction under visible light irradiation at room temperature and the system was open to air

The data are obtained following a two-step experiments. At first period the mixture of the catalyst and dye solution was stirred for 15 min in the dark and then the mixture was exposed to visible light. This result suggested that the MB

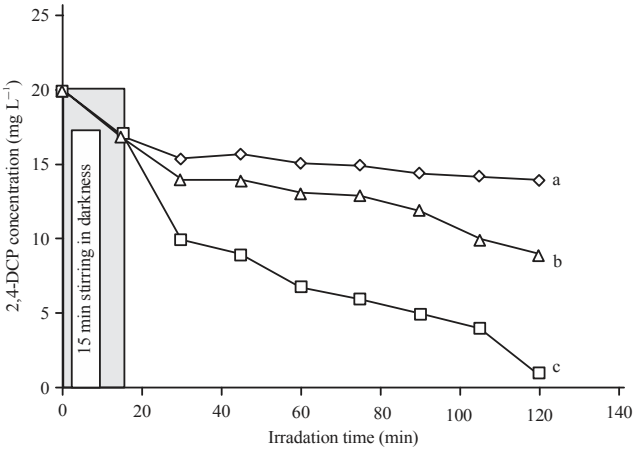

Fig. 7: Concentration changes of 2,4-DCP as a function of time using AG_3PO_4/MCM-41(PS) in various conditions, (a) Dark, (b) Irradiated by visible light and (c) Irradiated by UV-A light. The initial concentration of 2,4-DCP was 20 mg L^{-1}, weight of catalyst was 40 mg, volume of the dye solution 50 mL

dye was effectively decomposed with the assistance of the as-synthesized AG_3PO_4/MCM-41(PS). For comparison, the elimination of MB with AG_3PO_4 and MCM-41 nano-particles were also investigated under identical conditions. It is found that most of the adsorption of dyes occurs within 15 min and the AG_3PO_4/MCM-41(PS) nano-composite exhibited highest adsorption of MB compared to those of AG_3PO_4 and MCM-41. The higher adsorption of dyes could lead to the easier and faster photocatalytic degradation processes. The photocatalytic reactions are typically surface-based processes and the photocatalytic efficiency is closely related to the adsorption property of dyes on the surfaces of photocatalysts[25].

The pure MCM-41 has no photocatalytic activity and little reduction of MB is due to progressive adsorption of MB on the surface of MCM-41. Comparing with the pure MCM-41, AG_3PO_4 exhibited much higher photocatalytic activities and AG_3PO_4/MCM-41 exhibited the highest photo catalytic activity.

Photo catalytic degradation of 2,4-dichlorophenol was studied with AG_3PO_4/MCM-41(PS). The degradation rate was increased by increasing the amount of the photocatalyst. It found that an optimal catalyst dose is 40 mg/50 mL for DCP degradation. The effect of pH was also studied. It was found that a neutral or slightly acidic medium would be suitable. It selected pH 5 for DCP degradation. Figure 7 showed the concentration changes of DCP with time under different conditions. These conducted experiments indicate that the

Table 1: Rate constant (k_{obs}) and correlation coefficients for MB degradation

Temperature		Pseudo-1st		Pseudo-2nd	
(°C)	Sample	R^2	K_{obs} (min^{-1})	R^2	k_2 (g mg^{-1} min^{-1})
25	AG_3PO_4/MCM-41(PS)	0.6365	0.066	0.9934	1.423
25	AG_3PO_4/MCM-41(DS)	0.9415	0.0081	-	-
25	AG_3PO_4	0.9937	0.032	-	-
25	MCM-41	0.7454	0.0034	-	-

MB: Methylene blue

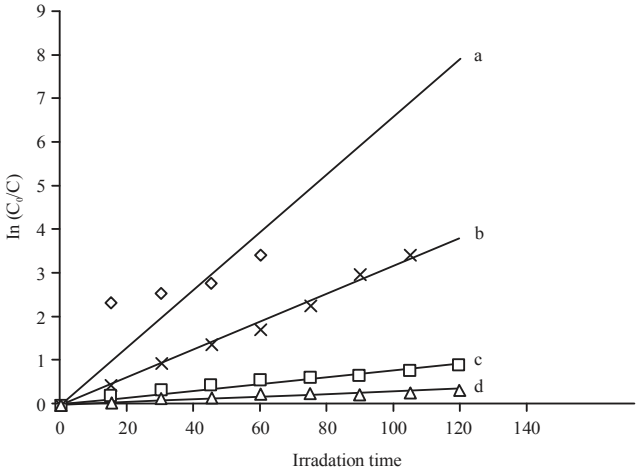

Fig. 8: Pseudo-first-order plot of (a) AG_3PO_4/MCM-41(PS), (b) AG_3PO_4, (c) AG_3PO_4/MCM-41(DS) and (d) MCM-41 for degradation of MB. The concentration of MB was 20 mg L^{-1}, weight of catalyst was 50 mg and volume of dye solution 50 mL, photocatalytic reaction under visible light irradiation at room temperature and the system was open to air

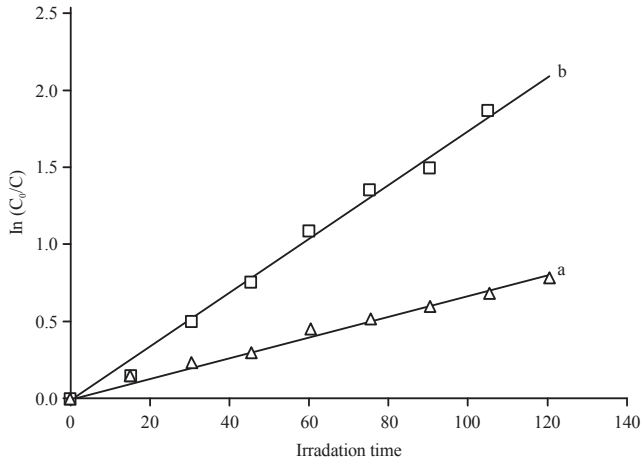

Fig. 9: Pseudo-first-order reaction of AG_3PO_4/MCM-41(PS) for degradation of 2,4-DCP (a) Under visible and (b) Under UV irradiation. The concentration of 2,4-DCP was 20 mg L^{-1}, the weight of catalyst was 40 mg, volume of the dye solution 50 mL

Table 2: Rate constant (k_{obs}) and correlation coefficients for 2,4-DCP degradation

K_{obs} (min^{-1})	R^2	Irradiation condition	Sample
0.0175	0.9931	UV light	AG_3PO_4/MCM-41(PS)
0.0068	0.9837	Visible light	AG_3PO_4/MCM-41(PS)
0.0036	0.9114	darkness	AG_3PO_4/MCM-41(PS)

light and catalyst are essential for efficient degradation of DCP (Fig. 7a). The degradation is more rapid when our source of krypton lamp is used instead of visible light.

The reaction rate plots were calculated for degradation of MB with the photocatalysts. The pseudo-first-order plots were shown in Fig. 8. The data should be fitted with $\ln (C_0/C) = k_{obs}t$ equation for a first-order kinetics. In this equation k_{obs} (min^{-1}) was the apparent rate constant, C_0 and C are the initial concentration and concentration at reaction time t for the probe molecule, respectively. The k_{obs} are calculated from the slopes of the straight lines obtained by plotting $\ln (C_0/C)$ versus irradiation time.

The results summarized in Table 1. The Table 1 showed that the correlation coefficients were very low for AG_3PO_4/MCM-41(PS) and MCM-41. This clearly indicated that the main reduction of MB in presence of AG_3PO_4/MCM-41(PS) is not due to photocatalytic degradation but because of adsorption. The correlation coefficient for this sample using a second-order reaction rate was also shown in Table 1. It was evident that the photocatalytic degradation of DCP with AG_3PO_4/MCM-41(PS) was fitted with a pseudo-first-order reaction (Fig. 9). The different behavior of AG_3PO_4/MCM-41(PS) for elimination of MB and DCP was probably due to presence of positive charge on MB and absence of charge on DCP. The kinetics results for 2,4-DCP were summarized in Table 2.

CONCLUSION

Two simple methods (post-synthesis and during-synthesis) were used for the preparation of AG_3PO_4/MCM-41. Parts of the formed AG_3PO_4 are embedded inside the pores as separate phase and parts of them most probably immobilized on the surface of MCM-41. Degradation of methylene blue and 2,4-dichlorophenol were investigated for evaluation of the photocatalysts.

SIGNIFICANCE STATEMENTS

The photo catalytic activity of the resulted AG_3PO_4/MCM-41 hetero-structures prepared via post-synthesis procedure was higher compared to that of AG_3PO_4/MCM-41 prepared during-synthesis of MCM-41. It is believed that MCM-41 provides appropriate vicinity for distribution of photo catalytically active AG_3PO_4 for designing a novel photocatalyst with high efficiency.

ACKNOWLEDGMENT

The research was supported by University of Guilan under Grant-1392-6. The authors are highly thankful to University of Guilan for providing financial assistance of this research project.

REFERENCES

1. Hernandez-Alonso, M.D., F. Fresno, S. Suarez and J.M. Coronado, 2009. Development of alternative photocatalysts to TiO_2: Challenges and opportunities. Energy Environ. Sci., 2: 1231-1257.
2. Sud, D. and P. Kaur, 2012. Heterogeneous photocatalytic degradation of selected organophosphate pesticides: A review. Crit. Rev. Environ. Sci. Technol., 42: 2365-2407.
3. Zhang, L., H. Wang, Z. Chen, P.K. Wong and J. Liu, 2011. Bi_2WO_6 micro/nano-structures: Synthesis, modifications and visible-light-driven photocatalytic applications. Applied Catal. B: Environ., 106: 1-13.
4. Tang, P., H. Chen and F. Cao, 2012. One-step preparation of bismuth tungstate nanodisks with visible-light photocatalytic activity. Mater. Lett., 68: 171-173.
5. Golmojdeh, H., M.A. Zanjanchi and M. Arvand, 2013. $BiVO_4$ Silica composites containing cobalt phthalocyanine groups: Synthesis, characterization and application in photodegradation of 2, 4, 6-Trichlorophenol. Photochem. Photobiol., 89: 1029-1037.
6. Xu, Y.H., C.J. Liu, M.J. Chen and Y.Q. Liu, 2011. A review in visible-light-driven $BiVO_4$ photocatalysts. Int. J. Nanoparticles, 4: 268-283.
7. Cui, C., Y. Wang, D. Liang, W. Cui and H. Hu *et al*., 2014. Photo-assisted synthesis of Ag_3PO_4/reduced graphene oxide/Ag heterostructure photocatalyst with enhanced photocatalytic activity and stability under visible light. Applied Catal. B: Environ., 158: 150-160.
8. Chen, X., Y. Dai and W. Huang, 2015. Novel $Ag_3PO_4/ZnFe_2O_4$ composite photocatalyst with enhanced visible light photocatalytic activity. Mater. Lett., 145: 125-128.
9. Guo, J., S. Ouyang, P. Li, Y. Zhang, T. Kako and J. Ye, 2013. A new heterojunction Ag_3PO_4/Cr-$SrTiO_3$ photocatalyst towards efficient elimination of gaseous organic pollutants under visible light irradiation. Applied Catal. B: Environ., 134: 286-292.
10. Liang, Q., W. Ma, Y. Shi, Z. Li and X. Yang, 2012. Hierarchical Ag_3PO_4 porous microcubes with enhanced photocatalytic properties synthesized with the assistance of trisodium citrate. CrystEngComm, 14: 2966-2973.
11. Zhang, H., H. Huang, H. Ming, H. Li, L. Zhang, Y. Liu and Z. Kang, 2012. Carbon quantum dots/Ag_3PO_4 complex photocatalysts with enhanced photocatalytic activity and stability under visible light. J. Mater. Chem., 22: 10501-10506.
12. Bi, Y., S. Ouyang, J. Cao and J. Ye, 2011. Facile synthesis of rhombic dodecahedral AgX/Ag_3PO_4 (X= Cl, Br, I) heterocrystals with enhanced photocatalytic properties and stabilities. Phys. Chem. Chem. Phys., 13: 10071-10075.
13. Yao, W., B. Zhang, C. Huang, C. Ma, X. Song and Q. Xu, 2012. Synthesis and characterization of high efficiency and stable Ag_3PO_4/TiO_2 visible light photocatalyst for the degradation of methylene blue and rhodamine B solutions. J. Mater. Chem., 22: 4050-4055.
14. Li, G. and L. Mao, 2012. Magnetically separable Fe_3O_4-Ag_3PO_4 sub-micrometre composite: Facile synthesis, high visible light-driven photocatalytic efficiency and good recyclability. RSC Adv., 2: 5108-5111.
15. Bi, Y., H. Hu, S. Ouyang, Z. Jiao, G. Lu and J. Ye, 2012. Selective growth of metallic Ag nanocrystals on Ag_3PO_4submicro cubes for photocatalytic applications. Chem.-A Eur. J., 18: 14272-14275.
16. Zhao, F.M., L. Pan, S. Wang, Q. Deng, J.J. Zou, L. Wang and X. Zhang, 2014. Ag_3PO_4/TiO_2 composite for efficient photodegradation of organic pollutants under visible light. Applied Surf. Sci., 317: 833-838.
17. Liu, R., P. Hu and S. Chen, 2012. Photocatalytic activity of Ag_3PO_4 nanoparticle/TiO_2 nanobelt heterostructures. Applied Surf. Sci., 258: 9805-9809.
18. Tang, C., E. Liu, J. Fan, X. Hu, L. Kang and J. Wan, 2014. Heterostructured Ag_3PO_4/TiO_2 nano-sheet film with high efficiency for photodegradation of methylene blue. Ceramics Int., 40: 15447-15453.
19. Schuth, F., 2001. Ordered mesoporous materials-state of the art and prospects. Stud. Surf. Sci. Catal., 135: 1-12.
20. Ciesla, U. and F. Schuth, 1999. Ordered mesoporous materials. Microporous Mesoporous Mater., 27: 131-149.
21. Zanjanchi, M.A. and S. Asgari, 2004. Incorporation of aluminum into the framework of mesoporous MCM-41: The contribution of diffuse reflectance spectroscopy. Solid State Ionics, 171: 277-282.

22. Beck, J.S., J.C. Vartuli, W.J. Roth, M.E. Leonowicz and C.T. Kresge *et al*., 1992. A new family of mesoporous molecular sieves prepared with liquid crystal templates. J. Am. Chem. Soc., 114: 10834-10843.
23. Coll, C., R. Martinez Manez, M.D. Marcos, F. Sancenon, J. Soto and R.K. Mahajan, 2009. Efficient removal of anionic surfactants using mesoporous functionalised hybrid materials. Eur. J. Inorg. Chem., 2009: 3770-3777.
24. Jaroniec, M., M. Kruk, H.J. Shin, R. Ryoo, Y. Sakamoto and O. Terasaki, 2001. Comprehensive characterization of highly ordered MCM-41 silicas using nitrogen adsorption, thermogravimetry, X-ray diffraction and transmission electron microscopy. Microporous Mesoporous Mater., 48: 127-134.
25. Tong, H., S. Ouyang, Y. Bi, N. Umezawa, M. Oshikiri and J. Ye, 2012. Nano-photocatalytic materials: Possibilities and challenges. Adv. Mater., 24: 229-251.